Development 135, 2127-2137 (2008) doi:10.1242/dev.020560

Selective expression of *Kras*^{G12D} in granulosa cells of the mouse ovary causes defects in follicle development and ovulation

Heng-Yu Fan[1], Masayuki Shimada[2], Zhilin Liu[1], Nicola Cahill[1], Noritaka Noma[2], Yun Wu[3], Jan Gossen[4] and JoAnne S. Richards[1,*]

Activation of the RAS family of small G-proteins is essential for follicle stimulating hormone-induced signaling events and the regulation of target genes in cultured granulosa cells. To analyze the functions of RAS protein in granulosa cells during ovarian follicular development in vivo, we generated conditional knock-in mouse models in which the granulosa cells express a constitutively active *Kras*^{G12D}. The *Kras*^{G12D} mutant mice were subfertile and exhibited signs of premature ovarian failure. The mutant ovaries contained numerous abnormal follicle-like structures that were devoid of mitotic and apoptotic cells and cells expressing granulosa cell-specific marker genes. Follicles that proceeded to the antral stage failed to ovulate and expressed reduced levels of ovulation-related genes. The human chorionic gonadotropin-stimulated phosphorylation of ERK1/2 was markedly reduced in mutant cells. Reduced ERK1/2 phosphorylation was due, in part, to increased expression of MKP3, an ERK1/2-specific phosphatase. By contrast, elevated levels of phospho-AKT were evident in granulosa cells of immature *Kras*^{G12D} mice, even in the absence of hormone treatments, and were associated with the progressive decline of FOXO1 in the abnormal follicle-like structures. Thus, inappropriate activation of KRAS in granulosa cells blocks the granulosa cell differentiation pathway, leading to the persistence of abnormal non-mitotic, non-apoptotic cells rather than tumorigenic cells. Moreover, those follicles that reach the antral stage exhibit impaired responses to hormones, leading to ovulation failure. Transient but not sustained activation of RAS in granulosa cells is therefore crucial for directing normal follicle development and initiating the ovulation process.

KEY WORDS: Ovary, Ovulation, Granulosa cell, *Kras* (*K-ras*), Signal transduction, MKP3 (DUSP6)

INTRODUCTION

Activation of small G-proteins within the RAS superfamily impact multiple downstream signaling cascades, including RAF1/MEK/ERK1/2 and PI3K/AKT/FOXO, in many tissues in a cell- and context-specific manner (Campbell et al., 2007; Cespedes et al., 2006; Gupta et al., 2007; Rocks et al., 2006). In response to growth-regulatory molecules, transient activation of RAS can stimulate controlled proliferation as well as differentiation of cells. Uncontrolled activation of RAS is often associated with oncogenic transformation or senescence of cells (Jackson et al., 2001; Lin et al., 1998; Serrano et al., 1997; Shaw et al., 2007). Specifically, RAS family members become oncogenic by single-point mutations, mainly at codons 12 or 13 (Bourne et al., 1990), leading to constitutive signaling and cell transformation with changes in morphology, increased proliferation and/or inhibition of apoptosis. Tissue-specific activation of oncogenic *Kras*^{G12D} causes mammary gland, lung and endometrioid ovarian carcinoma in mouse (Dinulescu et al., 2005; Jackson et al., 2001; Sarkisian et al., 2007). Mutations of *KRAS* or *BRAF* in non-invasive and invasive carcinomas of the ovary [involving the ovarian surface epithelium (OSE)] have been reported (Gemignani et al., 2003; Mayr et al., 2006).

In this study, we sought to determine the impact of RAS activation in granulosa cells in vivo. The constitutively active *Kras*^{G12D} mutation (Johnson et al., 2001) was selectively expressed in mouse granulosa cells using a Cre-mediated DNA recombination approach. The inappropriate, premature expression of *Kras*^{G12D} in granulosa cells blocked granulosa cell differentiation at an early stage, leading to the formation of abnormal follicle-like structures containing non-mitotic, non-apoptotic, non-differentiated and non-tumorigenic cells. Moreover, those follicles that reached the antral stage exhibited impaired responses to hormones, leading to ovulation failure. Thus, transient but not sustained activation of RAS in granulosa cells is crucial for normal follicle growth and successful completion of the ovulation process.

MATERIALS AND METHODS

Animals

LSL-Kras^{G12D}*;Amhr2-Cre* mice were derived from previously described *Amhr2-Cre* and *LSL-Kras*^{G12D} parental strains (Jamin et al., 2002; Tuveson et al., 2004). Although *Amhr2* is highly expressed in granulosa cells of growing follicles it is also known to be expressed in other reproductive tissues, including ovarian surface epithelial cells and the uterus (Arango et al., 2008) (our unpublished observations). Therefore, we sought to obtain a Cre-expressing mouse model that would be more highly specific for granulosa cells. *Cyp19-Cre* transgenic mice were generated by oocyte microinjection of a DNA fragment in which the 304 bp *Cyp19* promoter (GenBank S85356, bp –278 to +26) was ligated to *iCre* cDNA. To study ovarian responses to exogenous gonadotropins, 21-day-old immature females were analyzed to avoid the complexity of ovarian functions associated with estrous cycles and endogenous surges of gonadotropins. Specifically, immature mice were injected intraperitoneally (ip) with 4 IU eCG (equine chorionic gonadotropin;

[1]Department of Molecular and Cellular Biology, Baylor College of Medicine, Houston, TX77030, USA. [2]Department of Applied Animal Science, Graduate School of Biosphere Science, Hiroshima University, Higashi-Hiroshima, 739-8528, Japan. [3]Breast Cancer Center, Baylor College of Medicine, Houston, TX77030, USA. [4]NV Organon, part of the Schering-Plough Corporation, Target Discovery Oss, Molenstraat 110, 5340 BH Oss, The Netherlands.

*Author for correspondence (e-mail: joanner@bcm.edu)

Accepted 22 April 2008

Calbiochem) followed 48 hours later with 5 IU hCG (human chorionic gonadotropin; American Pharmaceutical Partners, Schaumburg, IL). Ovulated COCs were collected from oviducts 16 hours after hCG injection. Animals were treated in accordance with the NIH Guide for the Care and Use of Laboratory Animals.

Granulosa cell cultures

Undifferentiated granulosa cells were released from mouse antral follicles by puncturing with a 26.5-gauge needle. Cells were cultured at a density of 1×10^6 cells/ml in defined medium (DMEM:F12 containing penicillin and streptomycin) in 12-well culture dishes. Cells were cultured overnight to allow attachment to the culture dish and were infected with adenoviral vectors expressing Cre (Ad5-CMV-Cre, generated by the Vector Development Laboratory, Baylor College of Medicine) or GFP as the infection control. The infected cells were treated with or without FSH [NIH-FSH-16, National Hormone and Peptide Program (Al Parlow), Torrance, CA; 100 ng/ml] for time intervals designated in the figure legends.

BrdU incorporation and TUNEL assays

Mice were injected ip with 50 mg/kg of BrdU in PBS, and were killed 2 hours later. Ovaries were isolated and fixed with 4% paraformaldehyde (PFA) overnight. Incorporated BrdU was detected by immunohistochemistry using BrdU antibody according to manufacturer's instructions (Sigma, St Louis, MO). TUNEL assays were performed on PFA-fixed paraffin-embedded sections using the ApopTag Plus Peroxidase In Situ Apoptosis Detection Kit (Serologicals Corporation, Norcross, GA) according to manufacturer's instructions.

Immunohistochemistry and immunofluorescence

Immunohistochemistry was performed on 4% PFA-fixed paraffin-embedded 5-μm sections using the VectaStain Elite Avidin-Biotin Complex Kit as directed by the manufacturer (Vector Labs, Burlingame, CA). Sections were probed with primary antibodies against FOXO1 or PCNA (Cell Signaling, CA) and visualized using a 3,3V-Diaminobenzidine Peroxidase Substrate Kit (Vector Labs). For immunofluorescence, ovaries were PFA fixed, embedded in OCT compound (Sakura Finetek USA, Torrance, CA) and stored at –80°C before sectioning. Sections were probed with anti-KRAS (Santa Cruz Biotechnology, Santa Cruz, CA), anti-phospho-AKT, anti-phospho-ERK1/2, anti-cleaved caspase 3, or anti-phospho-histone H3 (Cell Signaling Technology) antibodies and visualized with Alexa Fluor 594-conjugated goat anti-rabbit IgG (Molecular Probes, Eugene, OR). Digital images were captured using a Zeiss Axiphot microscope with 5-40× objectives. For all the experiments, exposure time was kept the same for control and *Kras* mutant samples.

In situ hybridization

Plasmids for *Nr5a2* and *Cyp11a1* probes were as described previously (Boerboom et al., 2005; Falender et al., 2003). A cDNA fragment of *Mkp3* was amplified by RT-PCR from mouse ovary total cDNA and subcloned into the pCR-TOPO4 vector (Invitrogen, Carlsbad, CA). In situ hybridization was performed as previously reported (Falender et al., 2003; Hsieh et al., 2005). Tissue histology and the radioactive probe were visualized under light- and dark-field illumination, respectively.

RT-PCR and real-time RT-PCR

Reverse transcription (RT)-PCR was performed using the SuperScript One-Step RT-PCR System with the Platinum Taq Kit (Invitrogen) and 100 ng samples of ovarian total RNA that had been isolated using the RNeasy Mini Kit (Qiagen, Germantown, MD). Approximately 0.625 μCi of [α-^{32}P]dCTP (3000 Ci/mmol; MP Biomedicals, Irvine, CA) were added to each reaction to generate radioactive signals. Primer sequences and amplification conditions used are available upon request. Samples were separated by electrophoresis on 5% PAGE gels, dried and exposed to Biomax XAR film (Eastman Kodak, Rochester, NY) to generate the presented images.

Quantitative (q) RT-PCR was performed using the Rotor-Gene 3000 thermocycler (Corbett Research, Sydney, Australia). Relative levels of gene expression were normalized to β-actin.

RAS activity assay

The RAS-binding domain (RBD) of the mouse PI3K p110α subunit (PIK3CA; aa 220-311) (Rodriguez-Viciana et al., 1996) and of mouse RAF1 (aa 55-131) (Campbell-Valois and Michnick, 2007) were PCR amplified from a mouse ovary cDNA pool and subcloned into pGEX 4T1 vector. Recombinant GST-PI3K RBD and GST-RAF1 RBD were expressed in the

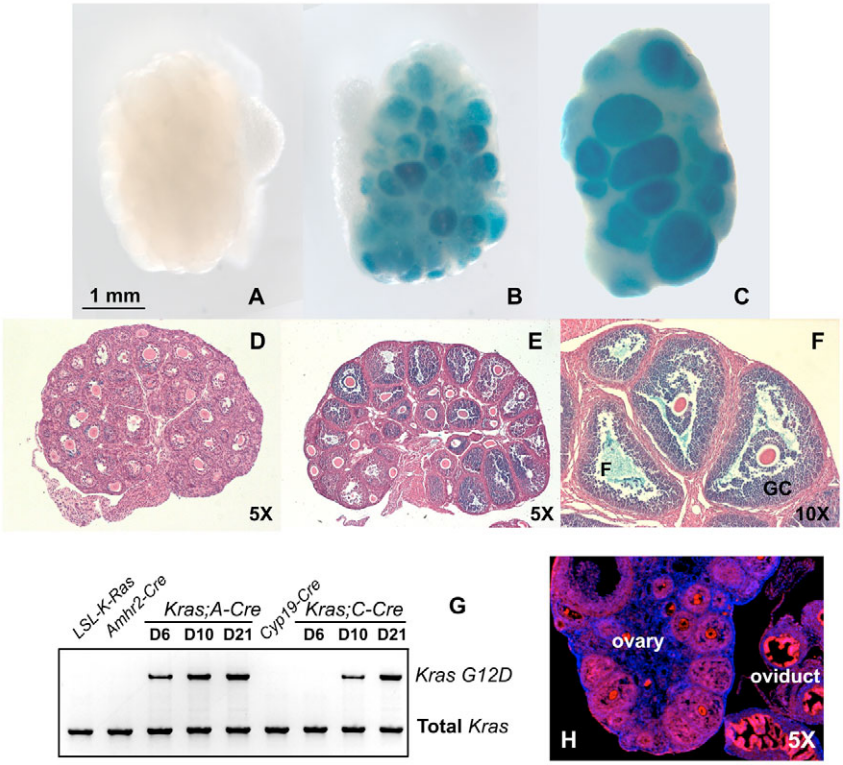

Fig. 1. Conditional knock-in of *Kras^{G12D}* in granulosa cells. (**A-F**) In vivo recombination of the *R26R* locus in ovaries by the *Cyp19-Cre* transgene. (A) *ROSA26*, (B) *ROSA26;Cyp19-Cre* and (C) *ROSA26;Cyp19-Cre*, 48 hours after eCG treatment. Images are of ovaries from 23-day-old mice showing β-gal staining (blue). (D) Day10 and (E) Day23 without eCG, and (F) Day23 with eCG treatment. Hematoxylin and Eosin staining of paraffin sections after β-gal staining showing the expression of β-gal in the ovaries of the *ROSA26;Cyp19-Cre* mouse. F, follicle; GC, granulosa cell. (**G**) RT-PCR detection of *Kras^{G12D}* and total *Kras* mRNAs in *LSL-Kras^{G12D};Amhr2-Cre* and *LSL-L-ras^{G12D};Cyp19-Cre* mouse ovaries. (**H**) Immunofluorescence of KRAS in the ovary of a 6-week-old cycling wild-type mouse.

Rosetta-pLysS *E. coli* strain (Novagen) and affinity purified using glutathione-agarose beads (Sigma). Ovaries were homogenized in lysis buffer (20 mM NaF, 10 mM $MgCl_2$, 100 mM NaCl, 10% glycerol, 0.5% Triton X-100, 20 mM HEPES, pH7.5). The lysates were incubated with agarose slurries linked with mouse RAF1 RBD or PI3K RBD to bind RAS-GTP. The agarose beads were washed and resuspended in Laemmli sample buffer prior to western blot analysis.

Western blot analysis

Western blots were performed utilizing 30 μg of lysate protein, 10% SDS-PAGE gels and transfer to Immobilin membrane (Millipore). Membranes were incubated with the following antibodies at 1:1000 dilutions: anti-phospho-FOXO1, anti-phospho-ERK1/2, anti-phospho-AKT, anti-AKT (all from Cell Signaling Technology) and anti-RAS (Upstate Biotechnology).

RNAi of *Mkp3*

Mkp3 siRNA (sc-39001) was purchased from Santa Cruz Biotechnology. Scrambled siRNA duplex (Ambion) was used as control. Transfection of siRNA (50 nM) into cultured granulosa cells was accomplished using the HVJ Envelope Vector Kit (Ishihara Sangyo, Tokyo, Japan) as previously reported (Shimada et al., 2007). The culture medium was replaced 5 hours after transfection and the cells were treated with 250 ng/ml amphiregulin (R&D Systems) for up to 4 hours.

RESULTS

Conditional knock-in of *Kras^{G12D}* in mouse ovarian granulosa cells

To induce the expression of $KRAS^{G12D}$ in granulosa cells, the previously described *LSL-Kras^{G12D}* mice were crossed with either the *Amhr2-Cre* knock-in mice (*Amhr2$^{cre/+}$*) (Jamin et al., 2002) or with transgenic mice in which Cre expression is driven by the *Cyp19* promoter (*Cyp19-Cre*). The ovarian expression pattern of the *Amhr2-Cre* allele has been described previously (Jorgez et al., 2004; Pangas et al., 2006; Boerboom et al., 2006). The generation of the *Cyp19-Cre* mouse strain is described in Materials and methods. To monitor the Cre activity in the ovaries, the *Cyp19-Cre* mice were crossed to the *ROSA26* reporter mouse strain that expresses β-galactosidase (β-gal) only in Cre-expressing cells (Soriano, 1999). Ovaries were stained for β-gal activity using X-Gal substrate as previously reported (Jorgez et al., 2004). No β-gal activity was detected in ovaries of *ROSA26* mice lacking Cre (Fig. 1A). In the *ROSA26;Cyp19-Cre* mice, β-gal was detected at low levels in granulosa cells of small follicles at postnatal day 10 (Fig. 1D) and at increased levels in granulosa cells of all antral follicles (Fig. 1B,E). Injections of *ROSA26;Cyp19-Cre* mice with equine chorionic gonadotropin (eCG), a known inducer of endogenous *Cyp19* expression, stimulated follicle growth and increased Cre activity (Fig. 1C,F). Cre activity was not detected in theca cells or oocytes throughout postnatal development (Fig. 1D-F). These results indicate that the *Cyp19-Cre* mouse strain exhibits specific expression of Cre in the granulosa cells, with minimal leakage in other cell types.

Examination of *Kras^{G12D}* mRNA in immature *LSL-Kras^{G12D};Amhr2-Cre* and *LSL-Kras^{G12D};Cyp19-Cre* mice demonstrated that the *Kras^{G12D}* allele was efficiently recombined and expressed at levels comparable to the endogenous *Kras* gene (Fig. 1G). Since endogenous KRAS protein is highly expressed in granulosa cells of growing follicles, expression of the mutant allele is being induced in the same cell type as the endogenous gene (Fig. 1H).

Granulosa cell expression of *Kras^{G12D}* impairs ovulation and female fertility

For fertility tests, *LSL-Kras^{G12D};Amhr2-Cre* and *LSL-Kras^{G12D};Cyp19-Cre* females were bred to wild-type males continuously for 6 months. The average number of ~7-8 pups per litter for the control mice (*LSL-Kras^{G12D}*) was not different from that of our C57BL/6J mouse colony. However, the *LSL-Kras^{G12D};Amhr2-Cre* and *Kras^{G12D};Cyp19-Cre* females (*n*=6, respectively) were subfertile over the 6-month period, with most pups being born in the first 2 months (Fig. 2A).

To determine the cause of reduced fertility in the *Kras^{G12D}* mutant mice, we tested their ability to ovulate by injecting immature mice with 4 IU of eCG and 46 hours later 5 IU of human chorionic gonadotropin (hCG). Whereas the control littermates ovulated many COCs at 16 hours after hCG injection, most *LSL-Kras^{G12D};Amhr2-Cre* mice did not ovulate at all, and only a few COCs were observed in the oviducts of *LSL-Kras^{G12D};Cyp19-Cre* mice (Fig. 2B). The

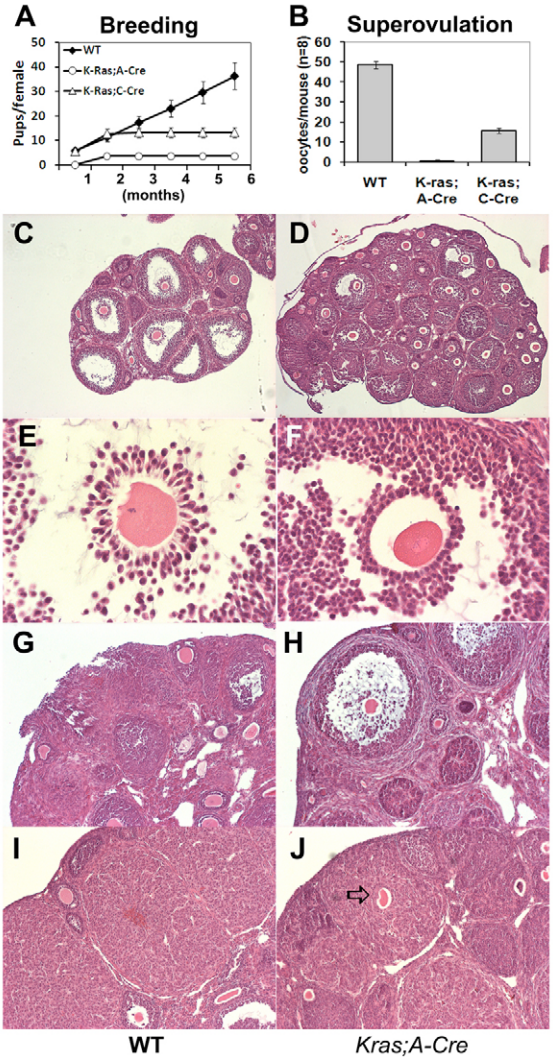

Fig. 2. Expression of $KRAS^{G12D}$ in granulosa cells causes multiple reproductive defects. (**A**) Continuous breeding assay showing the cumulative number of progeny per female. The *LSL-Kras^{G12D};Amhr2-Cre* and *LSL-Kras^{G12D};Cyp19-Cre* females (*n*=6) were subfertile. (**B**) Superovulation experiments showing that the ovulation rate in response to gonadotropins was reduced in *Kras* mutant mice (*n*=10) as compared with the wild type (WT). (**C-J**) Histology of WT (C,E,G,I) and *LSL-Kras^{G12D};Amhr2-Cre* (D,F,H,J) ovaries at 8 (C-F), 16 (G,H) and 48 (I,J) hours after hCG treatment. Histology of WT (I) and *LSL-Kras^{G12D};Amhr2-Cre* (J) ovaries 48 hours after hCG treatment shows that an oocyte is trapped in the corpus luteum of the *Kras* mutant ovary (arrow).

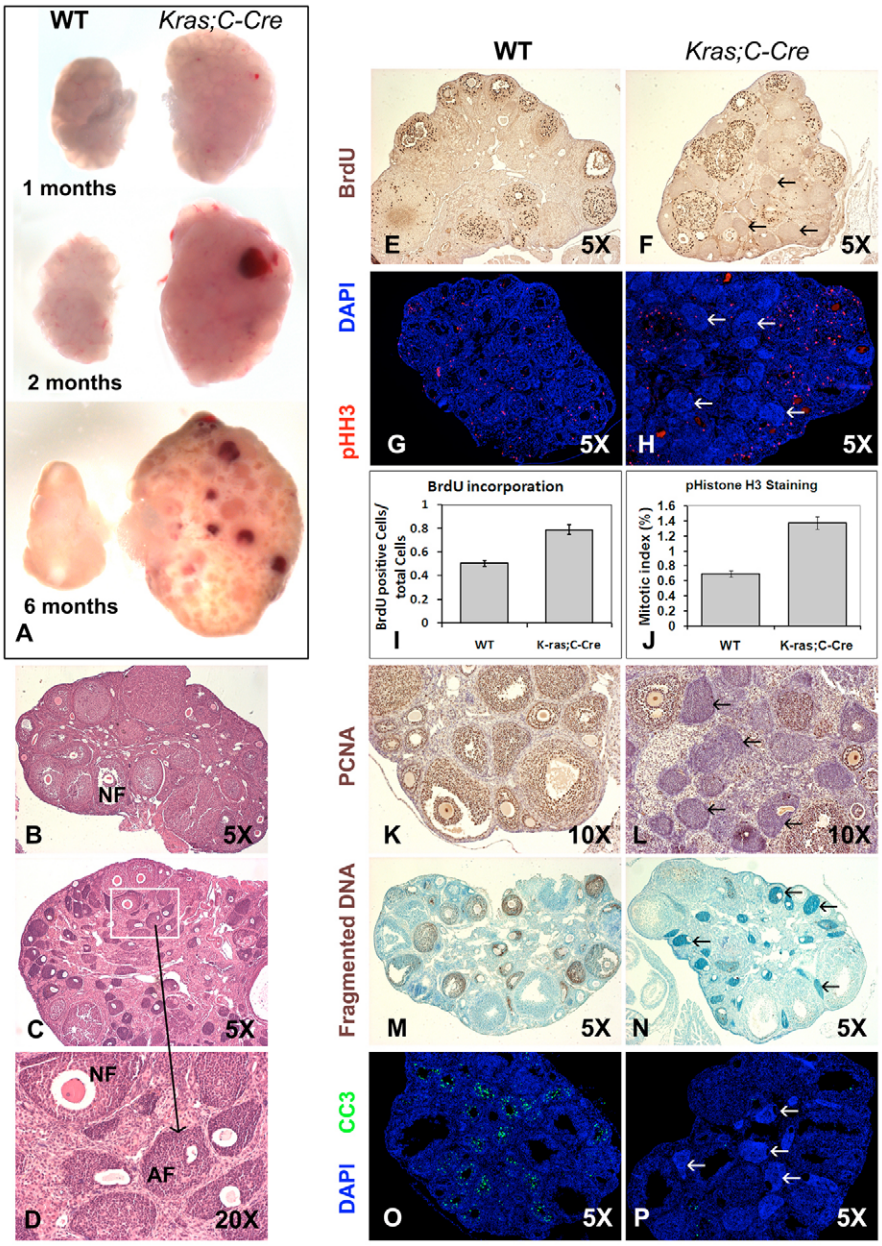

Fig. 3. *Kras^{G12D}* conditional knock-in mice develop ovarian lesions with altered granulosa cell proliferation, differentiation and apoptosis. (**A**) Size differences in wild-type (WT) and *LSL-Kras^{G12D};Cyp19-Cre* ovaries at various ages. (**B-D**) Histology of WT (B) and *LSL-Kras^{G12D};Cyp19-Cre* (C,D) ovaries at 6 months of age. NF, normal follicle; AF, abnormal follicle. (**E**,**F**) BrdU incorporation assay in 12-week-old WT (E) and *LSL-Kras^{G12D};Cyp19-Cre* (F) ovaries. Abnormal follicle-like structures are indicated by arrows (as below). (**G**,**H**) Immunofluorescent detection of phospho-histone H3 (pHH3, red) in 12-week-old WT (G) and *LSL-Kras^{G12D};Cyp19-Cre* (H) ovaries. (**I**,**J**) BrdU incorporation (I) and immunofluorescence for the mitosis marker phospho-histone H3 (J) indicate slightly increased levels of proliferation in *Kras^{G12D}*-expressing granulosa cells of antral follicles, as compared with wild type. (**K**,**L**) Immunohistochemical detection of PCNA in 12-week-old WT (K) and *LSL-Kras^{G12D};Cyp19-Cre* (L) ovaries. (**M**,**N**) Apoptosis assays in 4-week-old WT (M) and *LSL-Kras^{G12D};Cyp19-Cre* (N) ovaries, 2 hours after hCG treatment. (**O**,**P**) Immunofluorescent detection of cleaved caspase 3 (CC3) in 12-week-old WT (O) and *LSL-Kras^{G12D};Cyp19-Cre* (P) ovaries.

histological data from the *LSL-Kras^{G12D};Amhr2-Cre* mice are presented because the block of ovulation was more complete in this strain. However, the overall histological patterns in the two mutant strains were similar. Specifically, ovulation failure in the mutant mice was associated with defects of COC expansion and with the germinal vesicle breakdown of oocytes (Fig. 2D,F), whereas expanded COCs and meiotic oocytes with condensed chromosomes were present in the preovulatory follicles of control mice, at 8 hours post-hCG (Fig. 2C,E). In control mice, most large antral follicles ovulated by 16 hours after hCG (Fig. 2G) and had well developed corpora lutea (CLs) at 48 hours post-hCG (Fig. 2I). By contrast, antral follicles containing unovulated COCs remained in the mutant mouse ovaries at 16 hours post-hCG (Fig. 2H) and unovulated oocytes were trapped at the center of the CL at 48 hours post-hCG (Fig. 2J). More than 40 sections of *Kras^{G12D}* mutant ovaries (n=4) were examined, and trapped oocytes were present in 80-90% of the newly formed CLs. Because comparative analyses of the two mutant mouse strains revealed similar phenotypes and because expression of the *Cyp19-Cre* transgene is more specific for granulosa cells than is *Amhr2-Cre*, data from the *Kras^{G12D};Cyp19-Cre* mice (C-Cre) mice are presented.

Kras^{G12D} conditional knock-in mice develop abnormal follicle-like structures with altered granulosa cell proliferation and apoptosis

Ovaries from *LSL-Kras^{G12D};Amhr2-Cre* and *LSL-Kras^{G12D};Cyp19-Cre* mice were consistently larger and increased progressively in size, as compared with control littermates (Fig. 3A). Histological sections of the *Kras* mutant ovaries revealed multiple abnormal small ‘follicle-like’ structures compared with controls (Fig. 3, C and D compared with B). These small follicle-like structures lacked an antrum and consisted of nests of disorganized, pleiomorphic granulosa cells. Many of these structures contained an oocyte of abnormal appearance that was

displaced to the periphery of the 'follicle' rather than being central (Fig. 3D). Cells within these abnormal follicle-like structures failed to express the granulosa cell marker genes *Nr5a1* (see Fig. S1A-D in the supplementary material), *Cyp11a1* (see Fig. S1E-H in the supplementary material) and *Foxo1* (data not shown), indicating that normal granulosa cell differentiation had been blocked at an early stage of follicle growth.

To characterize the *Kras* mutant ovaries at the cellular level, we examined the proliferative rate of the developing follicles. In antral follicles, $Kras^{G12D}$-expressing granulosa cells demonstrated slightly increased levels of proliferation, based on BrdU incorporation (Fig. 3E,F,I) and immunofluorescence for the mitosis marker phospho-histone H3 (pHH3) (Fig. 3G,H,J). By contrast, only a limited number of cells within the abnormal follicle-like structures were positive for these proliferation markers. Immunohistochemical staining for proliferating cell nuclear antigen (PCNA) further proved that these abnormal structures are negative for proliferation markers (Fig. 3K,L).

Since the cells in the aberrant ovarian lesions were non-mitotic, the progressive enlargement of *Kras* mutant ovaries and the increased number of abnormal follicle-like structures might be caused by repression of apoptosis, a common feature in the mammalian ovary that serves to eliminate atretic follicles (Wang et al., 2006). Both the TUNEL assay and immunostaining for cleaved caspase 3 (CC3) were analyzed in the *Kras* mutant ovaries. Immature control and *Kras* mutant mice were primed with eCG and hCG to stimulate increased follicle growth. At 2 hours after hCG, DNA fragmentation (Fig. 3M) and caspase 3 cleavage (Fig. 3O) were detected in multiple pre- and early-antral follicles in control ovaries. By contrast, these apoptosis markers were markedly reduced in the *Kras* mutant ovaries, where the abnormal follicle-like structures were completely devoid of fragmented DNA and cleaved caspase 3 (Fig. 3N,P). These results show that apoptosis was repressed by the $Kras^{G12D}$ mutation in granulosa cells.

$Kras^{G12D}$ downregulates genes essential for granulosa cell differentiation and ovulation

Because the $Kras^{G12D}$ knock-in mice failed to ovulate, the expression of genes crucial for granulosa/cumulus cell differentiation and ovulation was analyzed in wild-type and mutant ovaries. As shown in Fig. 4A, *Fshr* mRNA was readily detected in ovaries of immature control mice and increased ~2.5-fold in response to eCG and was associated with the growth of preovulatory follicles. Other genes highly induced by eCG were *Lhcgr*, a marker of differentiated granulosa cells in preovulatory follicles, *Areg*, which encodes an EGF-like factor, and *Cyp11a1*, which encodes the steroidogenic enzyme leading to progesterone biosynthesis. Whereas expression of *Fshr* and *Lhcgr* was selectively reduced by the ovulatory stimulus of hCG, genes associated with ovulation (*Areg*, *Ptgs2* and *Tnfaip6*) and luteinization (*Cyp11a1*) were upregulated markedly by hCG (Fig. 4A). By contrast, the induced expression of these genes was reduced/altered in ovaries of the $Kras^{G12D}$ mutant mice. Notably, levels of *Fshr* mRNA were reduced in the ovaries of immature (untreated) *Kras* mutant mice indicating that constitutively active KRAS impairs the expression of this gene at an early stage of granulosa cell differentiation.

To determine whether the decreased levels of *Fshr* and *Lhcgr* mRNAs were the direct effect of mutant $Kras^{G12D}$ expression, we isolated undifferentiated granulosa cells from immature *LSL-*$Kras^{G12D}$ mice and cultured them in serum-free medium followed by infection with an adenoviral vector expressing Cre recombinase driven by the CMV promoter (Ad-CMV-Cre). In control cells,

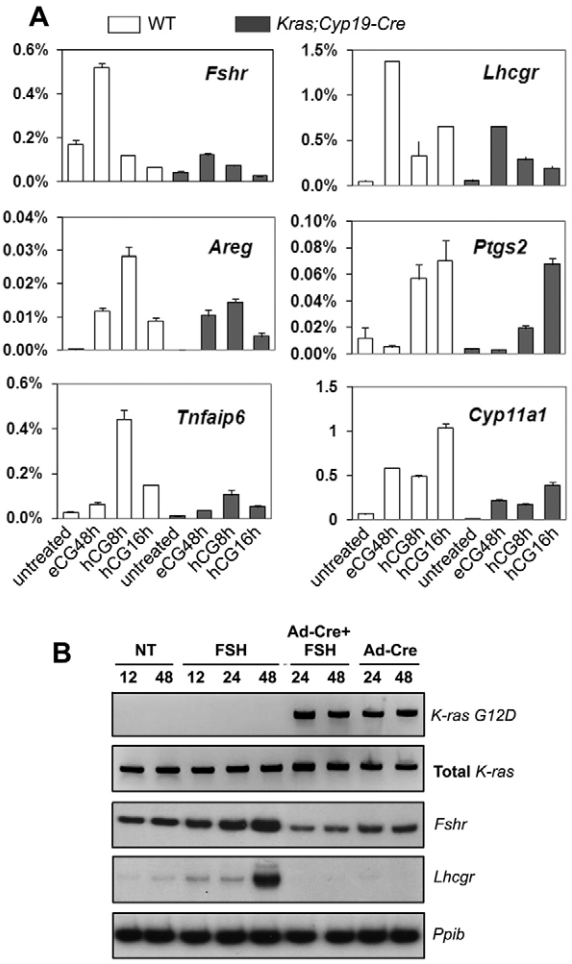

Fig. 4. $Kras^{G12D}$ downregulates genes essential for granulosa cell differentiation and ovulation. (**A**) qRT-PCR of ovulation-related genes from mouse whole ovary mRNAs. Six ovaries from different animals were analyzed. (**B**) $Kras^{G12D}$ downregulated the expression of *Fshr* and prevented the FSH-induced expression of *Lhcgr* in cultured granulosa cells. Expression of $Kras^{G12D}$ was induced by infecting the cells with an adenoviral vector encoding Cre recombinase (Ad-Cre). FSH (100 ng/ml) was added to the medium of cells infected, or not, with Ad-Cre. NT, non-treated. *Ppib* was amplified by RT-PCR in the same samples, as loading control.

addition of FSH to the medium upregulated *Fshr* and induced the expression of *Lhcgr* mRNAs. However, the *Fshr* mRNA level decreased in the granulosa cells expressing $Kras^{G12D}$, and the inductive effect of FSH on *Lhcgr* mRNA was totally abolished (Fig. 4B). This experiment confirmed our observations in vivo (Fig. 4A) and provided direct evidence that $KRAS^{G12D}$ reduces *Fshr* mRNA levels and blocks FSH-mediated induction of luteinizing hormone (LH) receptors in granulosa cells.

$KRAS^{G12D}$ activates both RAF1/MAPK and PI3K/AKT pathways in granulosa cells

FSH and LH transiently activate ERK1/2 and PI3K pathways in granulosa cells (Cottom et al., 2003; Gonzalez-Robayna et al., 2000). Recently, FSH has been shown to activate RAS, indicating that granulosa cells have factors that mediate G-protein receptor coupling to RAS (Wayne et al., 2007). Therefore, we analyzed components of the RAF1/MEK1/ERK1/2 and PI3K/AKT cascades

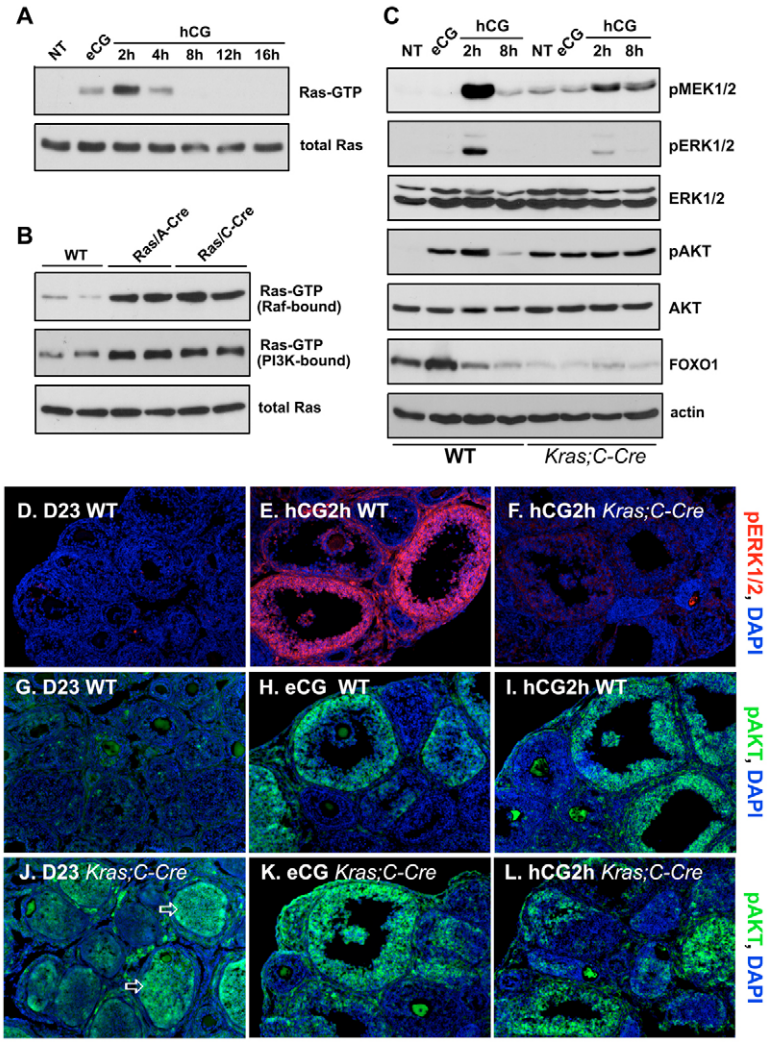

Fig. 5. KRAS^{G12D} activates the RAF1/MEK/ERK1/2 and PI3K/AKT pathways in granulosa cells. (**A**) RAS activity in wild-type ovaries during ovulation, as measured by a GST pull-down assay using RAF1 RAS-binding domain (RBD) as the bait. NT, non-treated. (**B**) RAS-GTP levels increased in immature *LSL-Kras^{G12D};Amhr2-Cre* and *LSL-Kras^{G12D};Cyp19-Cre* ovaries, as measured by the GST pull-down assay using both RAF1 RBD and p110α RBD. (**C**) Phosphorylation of MEK1/2, ERK1/2 and AKT in wild-type and *LSL-Kras^{G12D};Cyp19-Cre* ovaries after eCG/hCG treatment. Total ERK1/2 and AKT are shown as loading controls. (**D-F**) Localization of phospho-ERK1/2 in ovaries. The level of phospho-ERK1/2 was low in immature wild-type mouse ovaries (D), but was increased in the large antral follicles 2 hours after hCG injection (E). By contrast, the phospho-ERK1/2 level remained low in *LSL-Kras^{G12D};Cyp19-Cre* ovaries after the same treatment (F). (**G-I**) Immunofluorescence of phospho-AKT in wild-type ovaries. (G) Immature ovary; (H) 48 hours after eCG; (I) 2 hours after hCG. (**J-L**) Immunofluorescence of phospho-AKT in *LSL-Kras^{G12D};Cyp19-Cre* ovaries. (J) Immature ovary before eCG treatment (abnormal follicle-like structures indicated by arrows); (K) 48 hours after eCG treatment; (L) 2 hours after hCG treatment. Three to six ovaries from different animals of each genotype were analyzed in each of these experiments.

in both control and *Kras^{G12D}* mutant ovaries. First, we measured RAS activity by RAS-GTP pull-down assay. Whereas levels of total RAS did not change throughout the ovulation period, levels of active, GTP-bound RAS were undetectable in ovaries at postnatal day 23, increased slightly in response to eCG (48 hours) and then increased markedly (but transiently) 2 hours after hCG (Fig. 5A). When RAS-GTP was measured by GST-RAF1 and GST-p110α pull-down assays in *Kras* mutant ovaries, high levels of RAS-GTP were present compared with control mice (Fig. 5B). These results indicate that *Kras^{G12D}* mutant protein interacts with both PI3K and RAF1 in ovaries.

The phosphorylation status of selected RAS downstream kinases was also analyzed. Levels of phospho-MEK1/2 (MAP2K1/2 – Mouse Genome Informatics) and phospho-ERK1/2 were negligible in ovaries of immature mice prior to and 48 hours after eCG treatment (Fig. 5C; NT and eCG, respectively), increased dramatically 2 hours post-hCG and declined by 4 hours (see Fig. S2A in the supplementary material). Levels of phospho-AKT were low in ovaries of immature mice but increased markedly after eCG treatment. Phospho-AKT was further increased 2 hours post-hCG stimulation, was maintained at 4 hours (Fig. 5C and see Fig. S2A in the supplementary material) and returned to a basal level 8 hours post-hCG, a pattern similar to that of PDK1 (see Fig. S2A in the supplementary material). In addition, the total amount of the known AKT target, FOXO1, was reduced in *Kras* mutant ovaries compared with controls. The total amounts of ERK1/2 and AKT, as well as of actin (loading control), were not altered by gonadotropin treatment (Fig. 5C).

In comparison to their phosphorylation patterns in wild-type mice, elevated levels of phospho-MEK1/2 and phospho-AKT were observed in ovaries of *Kras* mutant mice even without hormonal stimulation (Fig. 5C, NT), and were only marginally increased in response to hCG, indicating that KRAS^{G12D} exerted stimulatory effects on these pathways (Fig. 5C). By contrast, the levels of phospho-ERK1/2 were undetectable in the same *Kras* mutant ovaries and increased only marginally after hCG treatment. These data suggested that potent inhibitory factors selectively reduced ERK1/2 phosphorylation.

To determine the cell-specific pattern of phospho-ERK1/2 and phospho-AKT in ovaries, immunofluorescent staining was performed using phospho-specific antibodies. In wild-type ovaries, phospho-ERK1/2 was only detected in the large antral follicles 2 hours after hCG (Fig. 5E and see Fig. S2B in the supplementary material). By contrast, levels of phospho-ERK1/2 were markedly reduced in *Kras* mutant ovaries treated in the same manner (Fig. 5F). In control ovaries, phospho-AKT was first detected after eCG stimulation in the mural layer of granulosa cells in the large antral follicles, whereas the signal was weak in the cumulus cells (Fig. 5H

and see Fig. S1C in the supplementary material). However, within 2 hours of hCG treatment, phospho-AKT was present in all granulosa/cumulus cells (Fig. 5I and see Fig. S1D in the supplementary material). By comparison, the phospho-AKT signal was already high in granulosa cells of the 23-day-old *Kras* mutant mice before eCG treatment. Phospho-AKT was also detected in some of the abnormal follicle-like structures (Fig. 5J, arrows). The progressive pattern of AKT phosphorylation was not seen in *Kras* mutant follicles. Rather, all granulosa/cumulus cells were positive for phospho-AKT after eCG treatment alone (Fig. 5K) or eCG/hCG treatment (2 hours) (Fig. 5L).

Acute effect of *Kras^{G12D}* expression in cultured granulosa cells

That KRAS^{G12D} interacts with RAF1 and activates MEK1/2 in granulosa cells but failed to increase ERK1/2 phosphorylation suggested that potent negative-feedback mechanisms were operative in these cells. To test this, granulosa cells isolated from 21-day-old *LSL-Kras^{G12D}* mouse ovaries were infected with Ad-CMV-Cre. Expression of *Kras^{G12D}* mRNA was detected by RT-PCR after adenoviral infection (Fig. 6A). Phospho-ERK1/2 increased gradually from 8 to 24 hours post-infection, but decreased to a basal level at 48 hours (Fig. 6B). Phospho-AKT also increased post-infection, but remained elevated at 48 hours, a time when the phospho-ERK1/2 level decreased, indicating that both the ERK1/2 and PI3K pathways in granulosa cells were transiently activated by KRAS^{G12D} but that negative-feedback mechanisms were induced to selectively block the ERK1/2 pathway in response to constitutively active KRAS^{G12D}. Additional *LSL-Kras^{G12D}* granulosa cells were infected with Ad-CMV-Cre or Ad-CMV-GFP (as control) for 48 hours and then stimulated with FSH, forskolin (Fo) or AREG for 20 minutes. As shown in Fig. 6C, each agonist induced ERK1/2 phosphorylation in control cells. However, in the cells expressing KRAS^{G12D}, the responses to agonists were markedly reduced indicating that KRAS^{G12D} activates a negative-feedback mechanism that represses ERK1/2 phosphorylation.

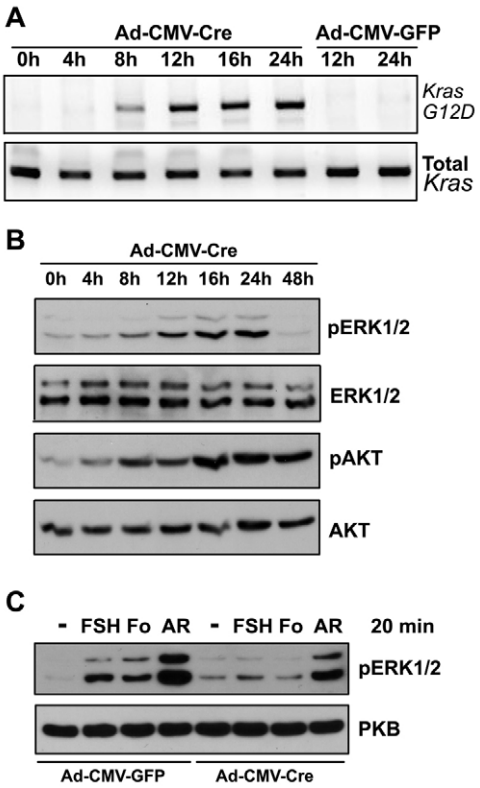

Fig. 6. Acute effect of *Kras^{G12D}* expression in cultured granulosa cells. (**A**) Expression of *Kras^{G12D}* mRNA in *LSL-Kras^{G12D}* granulosa cells after infection with Ad-CMV-Cre. (**B**) Levels of phospho-ERK1/2 and phospho-AKT post-infection. (**C**) *LSL-Kras^{G12D}* granulosa cells infected with Ad-CMV-Cre and control vectors (Ad-CMV-GFP) for 48 hours were stimulated with FSH, forskolin (Fo) or amphiregulin (AR) for 20 minutes. Each agonist induced ERK1/2 phosphorylation in control granulosa cells, but the responses were reduced in the cells expressing KRAS^{G12D}.

Mkp3 is upregulated by *Kras^{G12D}* in granulosa cells and negatively regulates ERK1/2 activity

To elucidate specific changes in ovarian gene expression associated with the *Kras^{G12D}* mutation, microarray analyses were undertaken using RNA prepared from ovaries of *LSL-Kras^{G12D};Amhr2-Cre* versus *LSL-Kras^{G12D}* mice at 26 days of age. The microarray data showed that the *Mkp3* (*Dusp6*) gene was upregulated in the *Kras* mutant ovaries, and this was confirmed by RT-PCR (Fig. 7A). This gene encodes MAPK phosphatase 3 (MKP3), which is an ERK1/2-specific protein phosphatase (Camps et al., 2000; Keyse, 2000; Li et al., 2007; Urness et al., 2007; Woods and Johnson, 2006). Expression of *Mkp3* was induced in granulosa cells both in vivo (2-4 hours) and in vitro (1-2 hours) by hCG and AREG stimulation, respectively (Fig. 7B,J). In situ hybridization showed that *Mkp3* mRNA is highly expressed in pre-ovulatory follicles 4 hours after hCG treatment (Fig. 7C,D), but is undetectable in 23-day-old ovaries (Fig. 7E,F). Ovaries of *LSL-Kras^{G12D};Amhr2-Cre* mice (23 days old) exhibited elevated expression of *Mkp3* mRNA in growing follicles, as compared with wild type (Fig. 7G,H, arrows).

To provide further evidence that MKP3 is functionally involved in the negative regulation of ERK1/2 activity, *Mkp3* mRNA was depleted in cultured granulosa cells by RNAi. *Mkp3* siRNA (50 nM) efficiently decreased *Mkp3* mRNA in unstimulated cells or those exposed to AREG, the most potent stimulator of ERK1/2 in granulosa cells (Fig. 7I). AREG induced rapid but transient phosphorylation of ERK1/2 in control granulosa cells. However, in cells treated with *Mkp3* siRNA, the dephosphorylation of ERK1/2 was significantly delayed (Fig. 7J,K). Lastly, ERK1/2 activity is required for the induction of *Mkp3*, because the MEK1/2 inhibitor PD98059 blocked the AREG-induced *Mkp3* expression in cultured granulosa cells (Fig. 7M,N).

DISCUSSION

Activation of the RAS small G-protein family is crucial for FSH and EGF-like factor-induced signaling events in cultured granulosa cells via stimulation of downstream kinases such as ERK1/2 and AKT (Wayne et al., 2007). Based on in vitro studies, the ERK1/2 pathway is presumed to be essential for COC expansion and meiotic resumption of oocytes (Diaz et al., 2006; Fan et al., 2003; Shimada et al., 2006; Su et al., 2002). FSH-mediated stimulation of the PI3K pathway is also presumed to impact follicular development (Alam et al., 2004; Alliston et al., 2000; Park et al., 2005; Richards et al., 2002; Zeleznik et al., 2003). By analyzing the effects of expressing a constitutively active form of KRAS (KRAS^{G12D}) selectively in granulosa cells of two mouse models, we report the first detailed investigation of the consequences of mutant KRAS activation during mammalian follicle development and ovulation. In both models, we observed two distinct follicular phenotypes, suggesting that the impact of *Kras^{G12D}* is dependent on the stage of granulosa cell

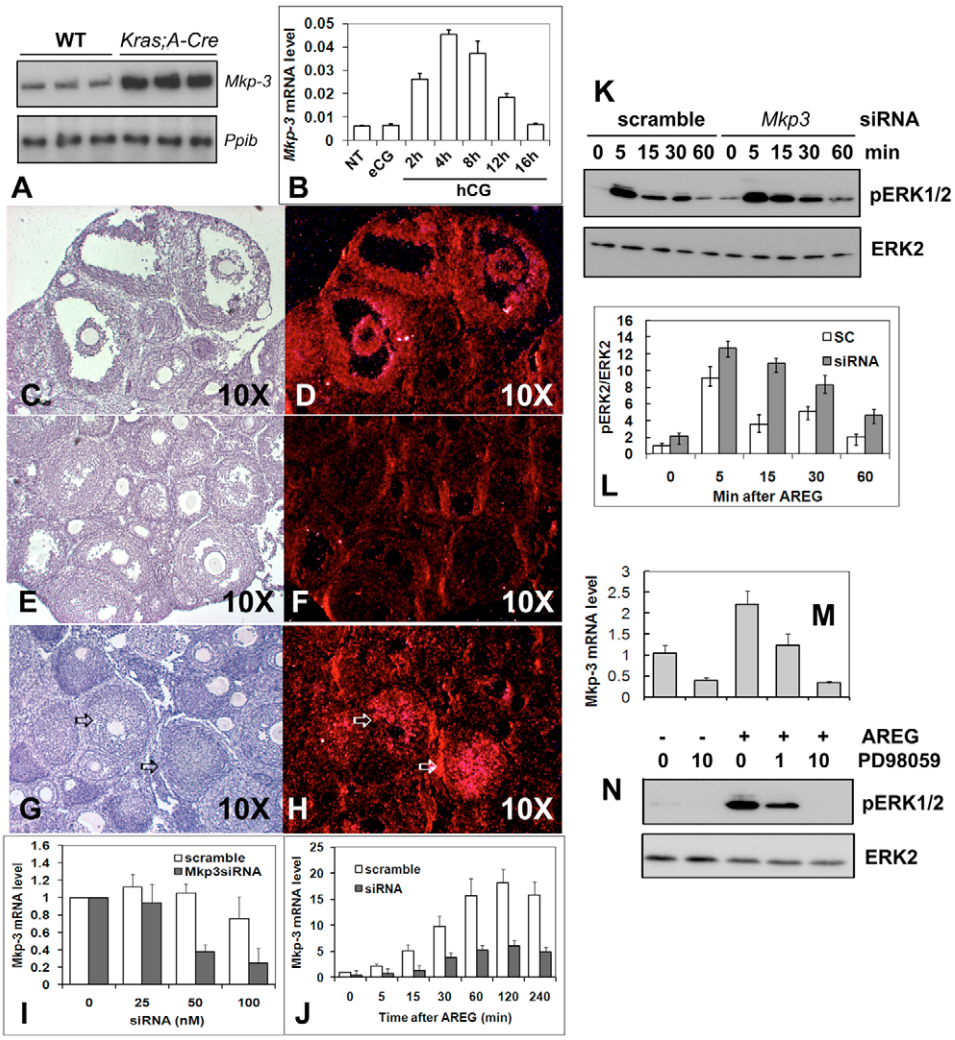

Fig. 7. *Mkp3* is a KRAS^{G12D}-induced gene involved in normal and abnormal granulosa cell development. (**A**) Semi-quantitive RT-PCR shows that *Mkp3* mRNA levels were elevated in *LSL-Kras^{G12D};Amhr2-Cre* ovaries as compared with those of wild-type mice (n=3 for each genotype). (**B**) *Mkp3* mRNA expression was induced in wild-type granulosa cells by eCG/hCG treatment. (**C-H**) In situ hybridization for *Mkp3* in wild-type and *Kras* mutant ovaries. Bright-field images show ovarian histology (C,E,G), whereas dark-field images show the signals of *Mkp3* antisense probe (D,F,H). *Mkp3* mRNA was detected in granulosa/cumulus cells at 4 hours after hCG (D), but not in immature wild-type ovaries (F). By contrast, *Mkp3* mRNA was detected in some preantral follicles (H, arrows) in *Kras* mutant ovaries of the same age. (**I**,**J**) *Mkp3* siRNA decreased the *Mkp3* mRNA levels in unstimulated granulosa cells (I) or those stimulated with AREG (J). (**K**,**L**) AREG induced transient phosphorylation of ERK1/2 in control granulosa cells; however, in the granulosa cells treated with *Mkp3* siRNA, levels of phospho-ERK1/2 remained elevated for longer (K). (L) Intensity comparison of phospho-ERK2/total ERK2. (**M**,**N**) PD98059 blocked AREG-induced *Mkp3* expression (M), when the ERK1/2 activation is blocked (N).

differentiation. If recombination occurred at early stages of follicle development, many abnormal follicle-like structures were observed, whereas if recombination occurred later, events associated with ovulation were impaired (Fig. 8). These changes in ovarian function caused the *Kras^{G12D}* mutant mice to be subfertile and to exhibit premature ovarian failure. Because *Amhr2-Cre* is expressed earlier in follicular development than *Cyp19-Cre* (our unpublished observations), the *Kras^{G12D};Amhr2-Cre* mice exhibited more-severe ovulation detects. The expression of the *Cyp19-Cre* transgene is highly specific for granulosa cells. Although *Cyp19-Cre* is expressed in follicles at slightly later stages of growth than *Amhr2-Cre*, the *Kras^{G12D};Cyp19-Cre* and *Kras^{G12D};Amhr2-Cre* phenotypes are very similar, verifying that mutant KRAS^{G12D} impacts granulosa cell function in a stage-specific manner.

Because granulosa cells are highly proliferative and KRAS^{G12D} can induce tumorigenic transformation of several cell types (Campbell et al., 2007; Sarkisian et al., 2007; Shaw et al., 2007; Tuveson et al., 2004), we anticipated that expression of KRAS^{G12D} in granulosa cells might lead to enhanced proliferation and oncogenic transformation of these cells. Oncogenic transformation was not observed and alterations in proliferation were critically dependent on when recombination and expression of KRAS^{G12D} were initiated. In the abnormal follicle-like structures, no evidence for proliferation was observed. However, in the large antral follicles, proliferation was increased, indicating that the effects of mutant KRAS were dependent on the stage of granulosa cell differentiation. Furthermore, expression of KRAS^{G12D} led to impaired apoptosis of granulosa cells in the abnormal follicle-like structures, whose growth appeared to be self-limiting. Expression of KRAS^{G12D} also profoundly altered the fate and differentiation of granulosa cells. Specifically, expression of mutant KRAS^{G12D} in granulosa cells of small growing follicles completely disrupted normal follicular development and granulosa cell differentiation, as known markers of granulosa cell function (*Fshr* and *Nr5a2*) (Richards, 1994) were not detected. This altered cell fate led to a novel and unexpected ovarian phenotype, with follicle-like structures that were devoid of mitotic, apoptotic and differentiated cells (Fig. 8). The behavior of the granulosa cells in these abnormal follicle-like structures appears to be similar to the premature senescence observed in primary cells in culture expressing mutant forms of HRAS (Lin et al., 1998).

Follicles in which granulosa cells escaped the recombination events at an early stage of development continued to grow to the antral stage. However, follicles with granulosa cells expressing KRAS^{G12D} at this stage also exhibited impaired function. Specifically, most antral follicles failed to ovulate even if exposed to exogenous hormones. Ovulation failure was associated with impairments in expansion of cumulus cells, in meiotic maturation of

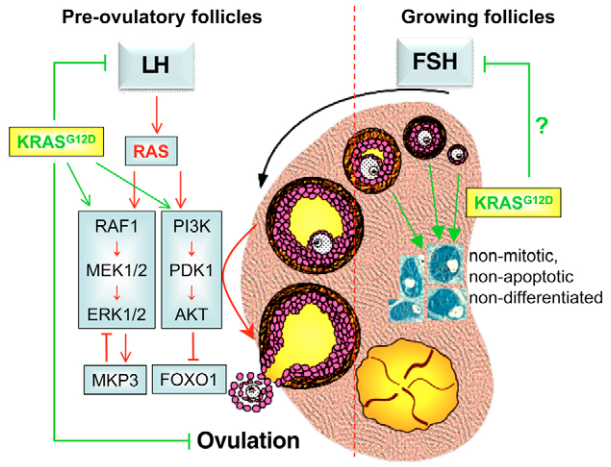

Fig. 8. Schematic of the ovarian defects caused by the expression of KRAS^{G12D} in developing follicles. In ovaries of wild-type mice, the LH/hCG surge transiently activates RAS and its downstream effecters, the ERK1/2 pathway and the PI3K pathway, which impact granulosa cell differentiation and ovulation by regulating the expression of numerous genes. ERK1/2 induces the expression of MKP3, which negatively regulates ERK1/2 activity in ovulating follicles as well as in cells expressing mutant *Kras^{G12D}*. PI3K regulates the phosphorylation of AKT and FOXO1. When KRAS^{G12D} is expressed in the granulosa cells, it interacts with both RAF1 and PI3K, activates ERK1/2 and AKT, respectively, and leads to two major ovarian phenotypes. In small follicles, the granulosa cells fail to differentiate and are devoid of their marker genes such as the FSH receptor. Moreover, these granulosa cells are non-mitotic, non-apoptotic and reside in abnormal follicle-like structures that accumulate in the ovaries of the mutant mice. Those follicles that escape this senescent fate develop to the antral stage but fail to ovulate because of the impaired expression of genes associated with ovulation. In addition, the mutant antral follicles exhibit reduced levels of phospho-ERK1/2 related to abnormally elevated levels of *Mkp3*. Red lines, RAS-related events in normal ovaries; green lines, KRAS^{G12D}-related events in mutant ovaries.

the oocytes and in expression of ovulation-related genes. This phenotype is similar to that of the mutant mouse model with an EGFR signaling defect (Hsieh et al., 2007). The altered response of KRAS^{G12D}-expressing granulosa cells to LH/hCG appears to be related to low levels of *Fshr* and the inability of FSH to induce expression of *Lhcgr* mRNA, and therefore to the loss of the crucial LH-ERK1/2 signaling pathways. This conclusion is supported by the reduced expression of specific genes known to be essential for COC expansion and ovulation (Richards, 2005), including *Ptgs2*, *Has2* and *Tnfaip6*.

The mechanisms by which KRAS^{G12D} alters granulosa cell functions and fate appear to be mediated by both the ERK1/2 pathway and the PI3K pathway. Specifically, our results show for the first time that treatment of mice in vivo with exogenous hormones, eCG and hCG, leads to transient activation of RAS and that this is associated with the transient phosphorylation of ERK1/2 and AKT in granulosa cells. By contrast, granulosa cells expressing KRAS^{G12D} exhibit elevated levels of RAS-GTP, as would be expected. In these cells, KRAS^{G12D} interacts with RAF1 and initially leads to increased phosphorylation of ERK1/2. These results support our recent study showing that RAS-GTP in rat granulosa cells interacts with RAF1 directly (Wayne et al., 2007), as well as the studies of others who have shown that KRAS^{G12D} selectively activates RAF1 and/or PI3K in a cell- and context-specific manner (Campbell et al., 2007; Cespedes et al., 2006; Gupta et al., 2007; Tuveson et al., 2004). However, KRAS^{G12D}-mediated ERK1/2 phosphorylation is transient and becomes markedly reduced in the mutant granulosa cells in vivo and in culture. This transient activation of ERK1/2 is mediated, at least in part, by the upregulation of MKP3, a specific ERK1/2 phosphatase (Camps et al., 2000; Keyse, 2000; Li et al., 2007; Urness et al., 2007; Woods and Johnson, 2006). *Mkp3* mRNA was rapidly induced in granulosa cells of wild-type mice in response to hCG and was elevated in *Kras^{G12D}* mutant ovaries (Fig. 7) and cultured granulosa cells expressing KRAS^{G12D} (data not shown). Because induction of *Mkp3* mRNA by AREG in granulosa cells was blocked by the MEK1/2 inhibitor PD98059, these results reinforce the notion that ERK1/2 induces expression of this negative-regulatory factor in granulosa cells. Conversely, reducing *Mkp3* expression by a siRNA approach prolonged the presence of phospho-ERK1/2 in response to AREG by up to 60 minutes. Collectively, these results provide evidence that MKP3 is regulated in murine ovarian granulosa cells and controls the duration of ERK1/2 phosphorylation.

Although *Mkp3* is induced in granulosa cells of preovulatory follicles and is initially elevated in these cells in the *Kras^{G12D}* mutant ovaries, *Mkp3* mRNA was not expressed in the granulosa cells contained within the abnormal follicle-like structures. Thus, the absence of phospho-ERK1/2 in these cells also indicates that other potent mechanisms impact and reduce ERK1/2 signaling in these mutant cells. For example, RAS can mediate the epigenetic silencing of genes via its ability to induce CpG methylation at promoter regions of certain genes (Gazin et al., 2007). Moreover, the mediators of RAS epigenetic silencing include *Mapk1* (*Erk2*), *Pdpk1* (*Pdk1*) and *Dnmt1* (Gazin et al., 2007). Thus, it is tempting to speculate that the cells within the abnormal follicle-like structures have undergone specific epigenetic changes to prevent their proliferation, apoptosis and differentiation.

In contrast to ERK1/2, phosphorylation of AKT in granulosa cells of growing and large antral follicles was enhanced by the presence of KRAS^{G12D} in vivo and in KRAS^{G12D}-expressing granulosa cells in culture. Since our GST pull-down assays showed that KRAS^{G12D} interacts directly with the p110α subunit of PI3K as previously reported (Rodriguez-Viciana et al., 1994; Rodriguez-Viciana et al., 1996), it is likely that KRAS^{G12D} stimulates the PI3K pathway directly, leading to the prolonged activation of AKT in granulosa cells. KRAS^{G12D} also impairs the expression of FOXO1 that may be mediated by prolonged activation of AKT. Since FOXO1 has been shown to impair granulosa cell differentiation (Park et al., 2005; Rudd et al., 2007), one might have predicted that the mutant cells would exhibit increased responsiveness to FSH, which is not the case. Rather, the PI3K pathway appears to regulate additional functions in granulosa cells. Because *Pdpk1* is a factor implicated in RAS-mediated epigenetic gene silencing (Gazin et al., 2007), it is possible that the PI3K pathway is crucial for dictating the fate of granulosa cells in small follicles.

In summary, transient activation of RAS and the phosphorylation of downstream targets, such as the RAF1/MEK1/ERK1/2 and PI3K/AKT cascades, appear to be crucial for mediating appropriate responses of granulosa cells to the gonadotropic hormones FSH and LH, leading to progressive follicular development and ovulation. Conversely, persistent expression of a constitutively active form of KRAS (KRAS^{G12D}) impairs ovulation and the expression of ovulation-related genes. Moreover, if expressed at an early stage in follicle development, KRAS^{G12D} dramatically alters granulosa cell fate by precluding granulosa cell differentiation, proliferation and apoptosis, thus impairing granulosa cell responses to gonadotropins

and leading to premature ovarian failure (Fig. 8). This marked divergence in granulosa cell function suggests that the potent epigenetic silencing of the promoters of specific genes might provide the basis of how activation of RAS alone can cause quiescence/senescence, rather than transformation, of these cells. These results also provide novel evidence that granulosa cells in vivo possess mechanisms that make them extremely impervious to tumorous transformation and that instead lead to premature ovarian failure.

We thank Dr Tyler Jacks for the *LSL-Kras^{G12D}* mice; Dr Richard Behringer for the *Amhr2-Cre* mice; Dr Michael Mancini and members of the Microscopy Core (HD-07495) for their time and assistance; and Yuet Lo for her many contributions. We thank Rebecca Robker and Darryl Russell for making the template of the ovary that appears in modified form in Fig. 8. This work is supported by NIH grants HD-16229 and HD-07495 (J.S.R.), and in part by JSPS-18688016 (M.S.). H.-Y.F. is supported in part by an NIH Postdoctoral Training Grant (HD-07165).

Supplementary material

Supplementary material for this article is available at http://dev.biologists.org/cgi/content/full/135/12/2127/DC1

References

Alam, H., Maizels, E. T., Park, Y., Ghaey, S., Feiger, Z. J., Chandel, N. S. and Hunzicker-Dunn, M. (2004). Follicle-stimulating hormone activation of hypoxia-inducible factor-1 by the phosphatidylinositol 3-kinase/AKT/Ras homolog enriched in brain (Rheb)/mammalian target of rapamycin (mTOR) pathway is necessary for induction of select protein markers of follicular differentiation. *J. Biol. Chem.* **279**, 19431-19440.

Alliston, T. N., Gonzalez-Robayna, I. J., Buse, P., Firestone, G. L. and Richards, J. S. (2000). Expression and localization of serum/glucocorticoid-induced kinase in the rat ovary: relation to follicular growth and differentiation. *Endocrinology* **141**, 385-395.

Arango, N. A., Kobayashi, A., Wang, Y., Jamin, S. P., Lee, H. H., Orvis, G. D. and Behringer, R. R. (2008). A mesenchymal perspective of mullerian duct differentiation and regression in Amhr2-lacZ mice. *Mol. Reprod. Dev.* **75**, 1154-1162.

Boerboom, D., Paquet, M., Hsieh, M., Liu, J., Jamin, S. P., Behringer, R. R., Sirois, J., Taketo, M. M. and Richards, J. S. (2005). Misregulated Wnt/beta-catenin signaling leads to ovarian granulosa cell tumor development. *Cancer Res.* **65**, 9206-9215.

Boerboom, D., White, L. D., Dalle, S., Courty, J. and Richards, J. S. (2006). Dominant-stable beta-catenin expression causes cell fate alterations and Wnt signaling antagonist expression in a murine granulosa cell tumor model. *Cancer Res.* **66**, 1964-1973.

Bourne, H. R., Sanders, D. A. and McCormick, F. (1990). The GTPase superfamily: a conserved switch for diverse cell functions. *Nature* **348**, 125-132.

Campbell, P. M., Groehler, A. L., Lee, K. M., Ouellette, M. M., Khazak, V. and Der, C. J. (2007). K-Ras promotes growth transformation and invasion of immortalized human pancreatic cells by Raf and phosphatidylinositol 3-kinase signaling. *Cancer Res.* **67**, 2098-2106.

Campbell-Valois, F. X. and Michnick, S. W. (2007). The transition state of the ras binding domain of Raf is structurally polarized based on Phi-values but is energetically diffuse. *J. Mol. Biol.* **365**, 1559-1577.

Camps, M., Nichols, A. and Arkinstall, S. (2000). Dual specificity phosphatases: a gene family for control of MAP kinase function. *FASEB J.* **14**, 6-16.

Cespedes, M. V., Sancho, F. J., Guerrero, S., Parreno, M., Casanova, I., Pavon, M. A., Marcuello, E., Trias, M., Cascante, M., Capella, G. et al. (2006). K-ras Asp12 mutant neither interacts with Raf, nor signals through Erk and is less tumorigenic than K-ras Val12. *Carcinogenesis* **27**, 2190-2200.

Cottom, J., Salvador, L. M., Maizels, E. T., Reierstad, S., Park, Y., Carr, D. W., Davare, M. A., Hell, J. W., Palmer, S. S., Dent, P. et al. (2003). Follicle-stimulating hormone activates extracellular signal-regulated kinase but not extracellular signal-regulated kinase kinase through a 100-kDa phosphotyrosine phosphatase. *J. Biol. Chem.* **278**, 7167-7179.

Diaz, F. J., O'Brien, M. J., Wigglesworth, K. and Eppig, J. J. (2006). The preantral granulosa cell to cumulus cell transition in the mouse ovary: development of competence to undergo expansion. *Dev. Biol.* **299**, 91-104.

Dinulescu, D. M., Ince, T. A., Quade, B. J., Shafer, S. A., Crowley, D. and Jacks, T. (2005). Role of K-ras and Pten in the development of mouse models of endometriosis and endometrioid ovarian cancer. *Nat. Med.* **11**, 63-70.

Falender, A. E., Lanz, R., Malenfant, D., Belanger, L. and Richards, J. S. (2003). Differential expression of steroidogenic factor-1 and FTF/LRH-1 in the rodent ovary. *Endocrinology* **144**, 3598-3610.

Fan, H. Y. and Sun, Q. Y. (2004). Involvement of mitogen-activated protein kinase cascade during oocyte maturation and fertilization in mammals. *Biol. Reprod.* **70**, 535-547.

Fan, H. Y., Tong, C., Lian, L., Li, S. W., Gao, W. X., Cheng, Y., Chen, D. Y., Schatten, H. and Sun, Q. Y. (2003). Characterization of ribosomal S6 protein kinase p90rsk during meiotic maturation and fertilization in pig oocytes: mitogen-activated protein kinase-associated activation and localization. *Biol. Reprod.* **68**, 968-977.

Gazin, C., Wajapeyee, N., Gobeil, S., Virbasius, C. M. and Green, M. R. (2007). An elaborate pathway required for Ras-mediated epigenetic silencing. *Nature* **449**, 1073-1077.

Gemignani, M. L., Schlaerth, A. C., Bogomolniy, F., Barakat, R. R., Lin, O., Soslow, R., Venkatraman, E. and Boyd, J. (2003). Role of KRAS and BRAF gene mutations in mucinous ovarian carcinoma. *Gynecol. Oncol.* **90**, 378-381.

Gonzalez-Robayna, I. J., Falender, A. E., Ochsner, S., Firestone, G. L. and Richards, J. S. (2000). Follicle-Stimulating hormone (FSH) stimulates phosphorylation and activation of protein kinase B (PKB/Akt) and serum and glucocorticoid-Induced kinase (Sgk): evidence for A kinase-independent signaling by FSH in granulosa cells. *Mol. Endocrinol.* **14**, 1283-1300.

Gupta, S., Ramjaun, A. R., Haiko, P., Wang, Y., Warne, P. H., Nicke, B., Nye, E., Stamp, G., Alitalo, K. and Downward, J. (2007). Binding of Ras to phosphoinositide 3-kinase p110alpha is required for Ras-driven tumorigenesis in mice. *Cell* **129**, 957-968.

Hsieh, M., Boerboom, D., Shimada, M., Lo, Y., Parlow, A. F., Luhmann, U. F., Berger, W. and Richards, J. S. (2005). Mice null for Frizzled4 (Fzd4$^{-/-}$) are infertile and exhibit impaired corpora lutea formation and function. *Biol. Reprod.* **73**, 1135-1146.

Hsieh, M., Lee, D., Panigone, S., Horner, K., Chen, R., Theologis, A., Lee, D. C., Threadgill, D. W. and Conti, M. (2007). Luteinizing hormone-dependent activation of the epidermal growth factor network is essential for ovulation. *Mol. Cell. Biol.* **27**, 1914-1924.

Jackson, E. L., Willis, N., Mercer, K., Bronson, R. T., Crowley, D., Montoya, R., Jacks, T. and Tuveson, D. A. (2001). Analysis of lung tumor initiation and progression using conditional expression of oncogenic K-ras. *Genes Dev.* **15**, 3243-3248.

Jamin, S. P., Arango, N. A., Mishina, Y., Hanks, M. C. and Behringer, R. R. (2002). Requirement of Bmpr1a for Mullerian duct regression during male sexual development. *Nat. Genet.* **32**, 408-410.

Johnson, L., Mercer, K., Greenbaum, D., Bronson, R. T., Crowley, D., Tuveson, D. A. and Jacks, T. (2001). Somatic activation of the K-ras oncogene causes early onset lung cancer in mice. *Nature* **410**, 1111-1116.

Jorgez, C. J., Klysik, M., Jamin, S. P., Behringer, R. R. and Matzuk, M. M. (2004). Granulosa cell-specific inactivation of follistatin causes female fertility defects. *Mol. Endocrinol.* **18**, 953-967.

Keyse, S. M. (2000). Protein phosphatases and the regulation of mitogen-activated protein kinase signalling. *Curr. Opin. Cell Biol.* **12**, 186-192.

Li, C., Scott, D. A., Hatch, E., Tian, X. and Mansour, S. L. (2007). Dusp6 (Mkp3) is a negative feedback regulator of FGF-stimulated ERK signaling during mouse development. *Development* **134**, 167-176.

Lin, A. W., Barradas, M., Stone, J. C., van Aelst, L., Serrano, M. and Lowe, S. W. (1998). Premature senescence involving p53 and p16 is activated in response to constitutive MEK/MAPK mitogenic signaling. *Genes Dev.* **12**, 3008-3019.

Mayr, D., Hirschmann, A., Lohrs, U. and Diebold, J. (2006). KRAS and BRAF mutations in ovarian tumors: a comprehensive study of invasive carcinomas, borderline tumors and extraovarian implants. *Gynecol. Oncol.* **103**, 883-887.

Pangas, S. A., Li, X., Robertson, E. J. and Matzuk, M. M. (2006). Premature luteinization and cumulus cell defects in ovarian-specific smad4 knockout mice. *Mol. Endocrinol.* **20**, 1406-1422.

Park, J. Y., Su, Y. Q., Ariga, M., Law, E., Jin, S. L. and Conti, M. (2004). EGF-like growth factors as mediators of LH action in the ovulatory follicle. *Science* **303**, 682-684.

Park, Y., Maizels, E. T., Feiger, Z. J., Alam, H., Peters, C. A., Woodruff, T. K., Unterman, T. G., Lee, E. J., Jameson, J. L. and Hunzicker-Dunn, M. (2005). Induction of cyclin D2 in rat granulosa cells requires FSH-dependent relief from FOXO1 repression coupled with positive signals from Smad. *J. Biol. Chem.* **280**, 9135-9148.

Richards, J. S. (1994). Hormonal control of gene expression in the ovary. *Endocr. Rev.* **15**, 725-751.

Richards, J. S. (2005). Ovulation: new factors that prepare the oocyte for fertilization. *Mol. Cell. Endocrinol.* **234**, 75-79.

Richards, J. S., Sharma, S. C., Falender, A. E. and Lo, Y. H. (2002). Expression of FKHR, FKHRL1, and AFX genes in the rodent ovary: evidence for regulation by IGF-I, estrogen, and the gonadotropins. *Mol. Endocrinol.* **16**, 580-599.

Rocks, O., Peyker, A. and Bastiaens, P. I. (2006). Spatio-temporal segregation of Ras signals: one ship, three anchors, many harbors. *Curr. Opin. Cell Biol.* **18**, 351-357.

Rodriguez-Viciana, P., Warne, P. H., Dhand, R., Vanhaesebroeck, B., Gout, I., Fry, M. J., Waterfield, M. D. and Downward, J. (1994). Phosphatidylinositol-3-OH kinase as a direct target of Ras. *Nature* **370**, 527-532.

Rodriguez-Viciana, P., Warne, P. H., Vanhaesebroeck, B., Waterfield, M. D. and Downward, J. (1996). Activation of phosphoinositide 3-kinase by interaction with Ras and by point mutation. *EMBO J.* **15**, 2442-2451.

Rudd, M. D., Gonzalez-Robayna, I., Hernandez-Gonzalez, I., Weigel, N. L., Bingman, W. E., 3rd and Richards, J. S. (2007). Constitutively active FOXO1a and a DNA-binding domain mutant exhibit distinct co-regulatory functions to enhance progesterone receptor A activity. *J. Mol. Endocrinol.* **38**, 673-690.

Sarkisian, C. J., Keister, B. A., Stairs, D. B., Boxer, R. B., Moody, S. E. and Chodosh, L. A. (2007). Dose-dependent oncogene-induced senescence in vivo and its evasion during mammary tumorigenesis. *Nat. Cell Biol.* **9**, 493-505.

Serrano, M., Lin, A. W., McCurrach, M. E., Beach, D. and Lowe, S. W. (1997). Oncogenic ras provokes premature cell senescence associated with accumulation of p53 and p16INK4a. *Cell* **88**, 593-602.

Shaw, A. T., Meissner, A., Dowdle, J. A., Crowley, D., Magendantz, M., Ouyang, C., Parisi, T., Rajagopal, J., Blank, L. J., Bronson, R. T. et al. (2007). Sprouty-2 regulates oncogenic K-ras in lung development and tumorigenesis. *Genes Dev.* **21**, 694-707.

Shimada, M., Hernandez-Gonzalez, I., Gonzalez-Robayna, I. and Richards, J. S. (2006). Paracrine and autocrine regulation of epidermal growth factor-like factors in cumulus oocyte complexes and granulosa cells: key roles for prostaglandin synthase 2 and progesterone receptor. *Mol. Endocrinol.* **20**, 1352-1365.

Shimada, M., Yanai, Y., Okazaki, T., Yamashita, Y., Sriraman, V., Wilson, M. C. and Richards, J. S. (2007). Synaptosomal-associated protein 25 gene expression is hormonally regulated during ovulation and is involved in cytokine/chemokine exocytosis from granulosa cells. *Mol. Endocrinol.* **21**, 2487-2502.

Soriano, P. (1999). Generalized lacZ expression with the ROSA26 Cre reporter strain. *Nat. Genet.* **21**, 70-71.

Su, Y. Q., Wigglesworth, K., Pendola, F. L., O'Brien, M. J. and Eppig, J. J. (2002). Mitogen-activated protein kinase activity in cumulus cells is essential for gonadotropin-induced oocyte meiotic resumption and cumulus expansion in the mouse. *Endocrinology* **143**, 2221-2232.

Tuveson, D. A., Shaw, A. T., Willis, N. A., Silver, D. P., Jackson, E. L., Chang, S., Mercer, K. L., Grochow, R., Hock, H., Crowley, D. et al. (2004). Endogenous oncogenic K-ras(G12D) stimulates proliferation and widespread neoplastic and developmental defects. *Cancer Cell* **5**, 375-387.

Urness, L. D., Li, C., Wang, X. and Mansour, S. L. (2007). Expression of ERK signaling inhibitors Dusp6, Dusp7, and Dusp9 during mouse ear development. *Dev. Dyn.* **237**, 163-169.

Wang, H., Jiang, J. Y., Zhu, C., Peng, C. and Tsang, B. K. (2006). Role and regulation of nodal/activin receptor-like kinase 7 signaling pathway in the control of ovarian follicular atresia. *Mol. Endocrinol.* **20**, 2469-2482.

Wayne, C. M., Fan, H. Y., Cheng, X. and Richards, J. S. (2007). Follicle-stimulating hormone induces multiple signaling cascades: evidence that activation of Rous sarcoma oncogene, RAS, and the epidermal growth factor receptor are critical for granulosa cell differentiation. *Mol. Endocrinol.* **21**, 1940-1957.

Woods, D. C. and Johnson, A. L. (2006). Phosphatase activation by epidermal growth factor family ligands regulates extracellular regulated kinase signaling in undifferentiated hen granulosa cells. *Endocrinology* **147**, 4931-4940.

Zeleznik, A. J., Saxena, D. and Little-Ihrig, L. (2003). Protein kinase B is obligatory for follicle-stimulating hormone-induced granulosa cell differentiation. *Endocrinology* **144**, 3985-3994.